Available online at www.sciencedirect.com
SCIENCE DIRECT®
Thin Solid Films 436 (2003) 238–243
thin solid films
www.elsevier.com/locate/tsf

Effect of metal vapor vacuum arc Cr-implanted interlayers on the microstructure of CrN film on silicon

Sheng Han[b], Hong-Ying Chen[c], Zue-Chin Chang[c], Jian-Hong Lin[a], Ching-Jung Yang[c], Fu-Hsing Lu[c], Fuh-Sheng Shieu[c], Han C. Shih[a,c,*]

[a]*Department of Materials Science and Engineering, National Tsing Hua University, 101 Kuang Fu Rd., Sec. 2, Hsinchu, Taiwan 300, ROC*
[b]*National Taichung Institute of Technology, 129 San-Min Rd., Sec. 3, Taichung, Taiwan 404, ROC*
[c]*Department of Materials Engineering, National Chung Hsing University, 250 Kuo Kuang Rd., Taichung, Taiwan 402, ROC*

Received 10 July 2002; received in revised form 27 February 2003; accepted 25 March 2003

Abstract

The effect of metal vapor vacuum arc (MEVVA) Cr-implanted interlayers on the microstructure of CrN films on the silicon wafer was investigated. Two types of the CrN-coated specimens (CrN/Si and CrN/Cr/Si) by cathodic arc plasma deposition were prepared with and without a MEVVA Cr-implanted interlayer. The diffraction patterns of the coated specimens revealed the presence of CrN, and the (220) preferred orientation for both CrN/Si and CrN/CrN/Si. The CrN coating thicknesses for CrN/Si and for CrN/Cr/Si were 0.3 μm and 1.3 μm, respectively. Secondary ion mass spectrometry proved the high quality of the films on silicon substrates. Transmission electron microscopy micrographs and selective area diffractions revealed the presence of a large number of nano-scale Cr resulting from the interlayer of MEVVA Cr with a background of single crystal silicon spots. Furthermore, in situ stress measurement demonstrated that the presence of a Cr interlayer between CrN and Si could drastically reduce the residual stress in the CrN/Cr/Si assembly.
© 2003 Elsevier Science B.V. All rights reserved.

Keywords: Metal vapor vacuum arc; Secondary ion mass spectrometry; Transmission electron microscopy; Residual stress

1. Introduction

Chromium nitride (CrN) films have been successfully applied in tools because of their excellent mechanical properties and corrosion resistance [1–3]. In our previous studies, a Cr interlayer was electroplated to increase the corrosion and tribological resistance of CrN films [1]. However, the electroplating industry is notorious for its pollution of the environment and the residual stress in this material system interlayer has seldom been investigated. Thus, this study employed metal vapor vacuum arc (MEVVA) ion implantation to deposit an interlayer of Cr. This method has many outstanding advantages, such as the ability to produce almost all species of metal ion, a very high current, pure ion beams, reasonably high charge states and a large beam spot [4]. This technique also allows the use of cathodic arc plasma deposition (CAPD) for forming CrN [5], and this study employs silicon wafers as the substrate. Two specimens were prepared; one was a pre-coated interlayer of Cr between the CrN film and the Si substrate, designated as CrN/Cr/Si and the other was CrN directly deposited on the Si substrate, designated as CrN/Si. The in situ residual stress measurements [6] were made to investigate the effect of an interlayer Cr on the residual stress. Understanding the effect of residual stress is useful in further studies.

2. Experimental details

A 725 μm thick p-type (100) Si wafer (Toshiba Ceramics Co., Ltd.) was selected as a substrate. The Cr interlayer was deposited using an MEVVA ion implanter at an extracting voltage of 50 kV. Nevertheless, the extracted Cr ions have various valencies, including Cr^{+}, Cr^{2+}, Cr^{3+} and Cr^{+4} [7]. The main component

*Corresponding author: Tel.: +886-3-571-5131 ext. 3845; fax: +886-3-571-0290.
E-mail address: hcshih@mse.nthu.edu.tw (H.C. Shih).

0040-6090/03/$ - see front matter © 2003 Elsevier Science B.V. All rights reserved.
PII: S0040-6090(03)00600-X

was Cr^{2+} with a corresponding average energy of 100 keV. The ion doses and the current density were 2×10^{17} ions/cm^2 and 6 μA/cm^2, respectively. The substrate temperature was measured by K-type thermocouples and the substrate was heated from nominal room temperature up to approximately 100 °C after implantation. A CAPD technique was used to produce CrN films. During the deposition, the substrate temperature was maintained at ∼350 °C at a bias of −150 V; the arc current was 60 A; the N_2 partial pressure was controlled at ∼3 Pa, and the deposition time was 70 min.

The crystal structures of CrN/Si and CrN/Cr/Si assemblies were investigated by X-ray diffraction (XRD) and transmission electron microscopy (TEM). A Mac Science MXP3 diffractometer using Cu K_α radiation ($\lambda=0.154$ nm) with the collected interval of 0.02°/2θ was used. A Philips CM2 TEM operating at 200 kV was used to examine the crystal structure of the Cr/Si assembly. The surface morphology and the thickness were measured by scanning electron microscopy (SEM), JEOL JSM-5400, operating at 15 kV. A Cameca IMS-4F secondary ion mass spectrometer (SIMS) with a Cs^+ primary beam with an impact energy of 14.5 keV and a primary current of 50 nA traced the depth profiles of chromium, nitrogen and silicon in the films. In situ curvature measurements were made using a scanning laser curvature method to determine the stress changes in the film. A He–Ne laser with a wavelength of 632.8 nm and a power of 7 mW was used. The laser spot was approximately 0.25 cm and moved through 1 cm on the surface of specimen. The curvature ($1/R$) of the film was obtained and the residual stress (σ_f) calculated using the Stoney's equation [8]:

$$\sigma_f=\frac{E_S}{6(1-\nu_S)}\times\frac{t_S^2}{t_f}\times\left(\frac{1}{R}\right) \quad (1)$$

where ν_S is the Poisson ratio of the substrate; E_S is Young's modulus of the substrate; t_f is the thickness of the film, and t_S the thickness of the substrate.

3. Results and discussion

3.1. XRD results

Firstly, XRD was used to examine the crystal structure of CrN/Si and of CrN/Cr/Si assemblies, as shown in Fig. 1. The two assemblies match the CrN phase as given in the JCPDS card [9]. Notably, the 2θ value of 33.01° is attributed to the second reflection from the Si substrate. The (200) and (220) diffraction line of the CrN phase is observed for both samples. Furthermore, the predominance of CrN (220) is the preferred orientation after the JCPDS card is compared with [9]. Such an obtained (220) orientation has a slightly lower

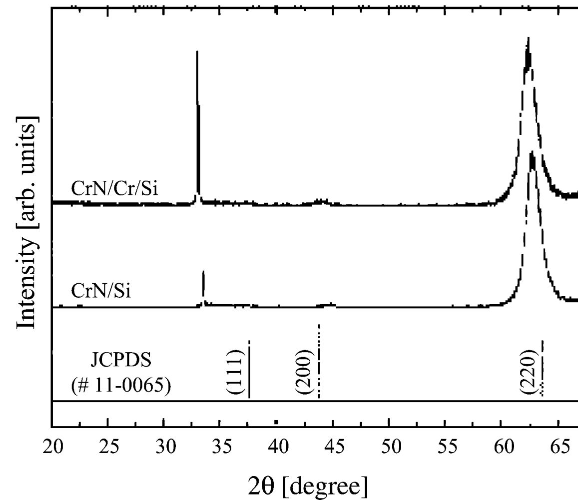

Fig. 1. XRD patterns of CrN/Si and CrN/Cr/Si showing a pronounced preferred orientation of (220).

diffraction angle, indicating a compressive residual stress in the film, which deserves to be examined further using a scanning laser curvature measurement. The full width at half maximum (FWHM) of the diffraction peak normally represents the grain size in Scherrer's equation. The grain sizes of the CrN/Si and CrN/Cr/Si assemblies are similar because of the similarity of the two FWHMs (1.47 vs. 1.74). The Cr interlayer does not affect the preferred orientation of the CrN films; this fact is consistent with the authors' previous studies on electroplated Cr as an interlayer [5].

3.2. SEM observation

Fig. 2 presents the SEM morphologies of the scattering of macroparticles on the surface films of the CrN/Si and CrN/Cr/Si assemblies. Macroparticles may result from the reactive force of intensive ions that flow back from the ionization region onto the underlying liquid pool of the chromium target, or from the plasma-generated micro-explosions on the cathode surface [10]. The macroparticles revealed by EDS consist of pure chromium. Fig. 2a,b depicts the decohesion of macroparticles at the particle-matrix interface while Fig. 2c,d shows the cross-sectional morphologies of the CrN/Si and CrN/Cr/Si assemblies. The surface morphologies are essentially the same and independent of the Cr interlayer. However, the difference in CrN film thickness, 0.3 μm for CrN/Si and 1.3 μm for CrN/Cr/Si, can be explained by the fact that the Cr ions implanted interlayer facilitates the nucleation and growth of CrN, which result in contrast to the results of our previous studies on the use of electroplated Cr to bridge the succeeding CrN coating resulting in well-textured forms [5].

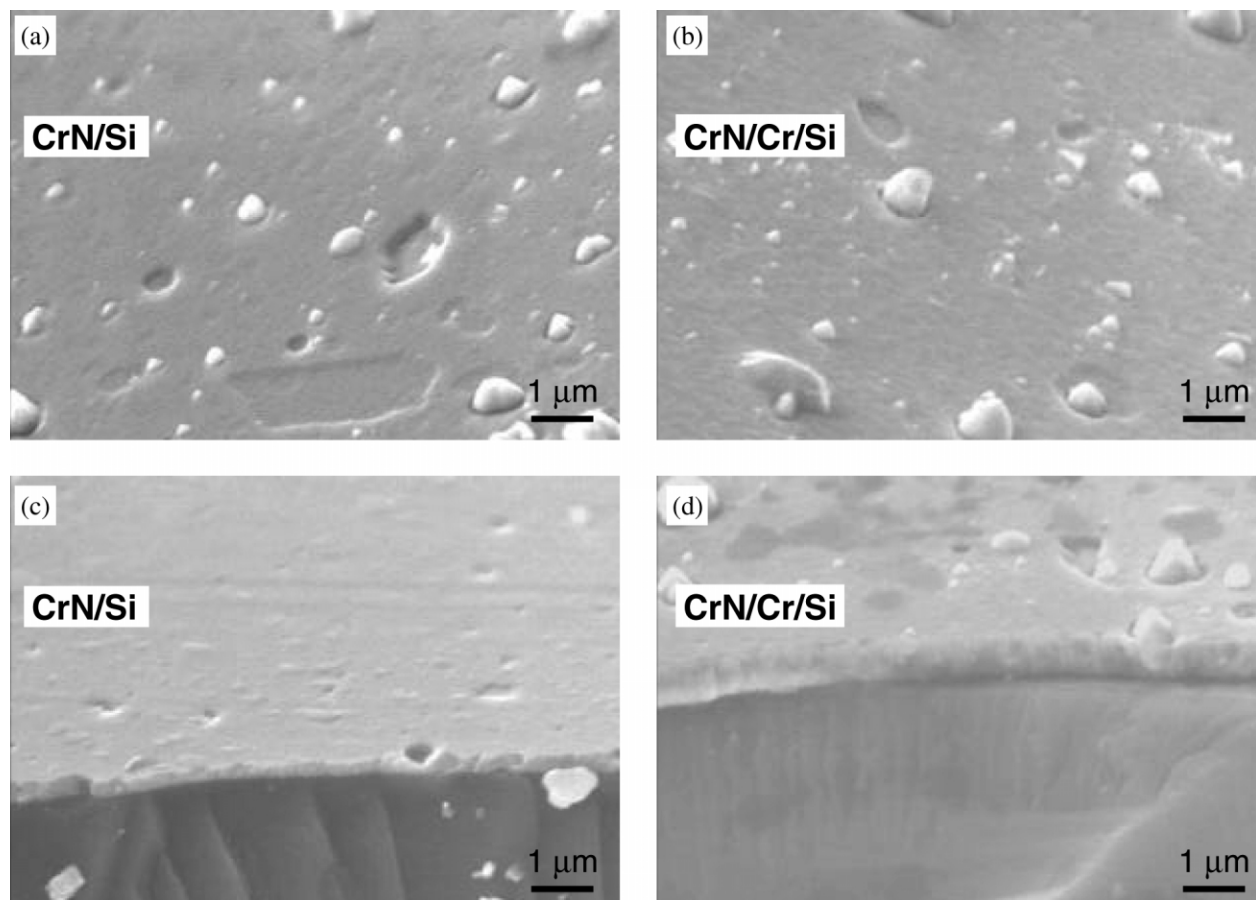

Fig. 2. SEM surface morphology of the films: (a) CrN/Si; and (b) CrN/Cr/Si and the corresponding SEM cross sectional morphology of the films: (c) CrN/Si; and (d) CrN/Cr/Si.

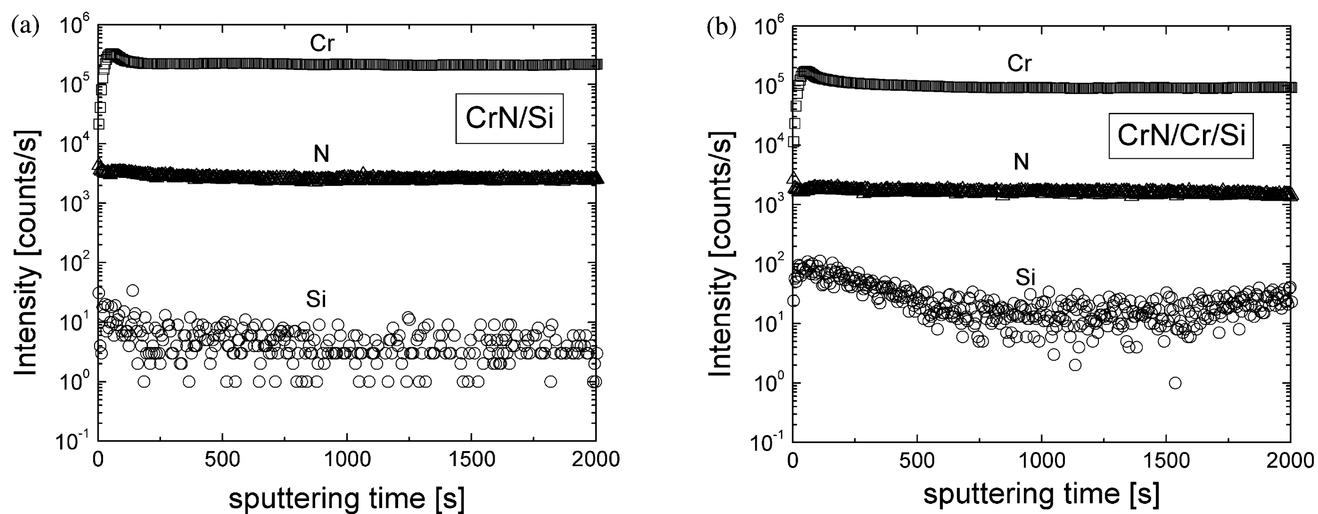

Fig. 3. The depth profile of elemental Cr, N, and Si as a function of sputtering time for (a) CrN/Si and (b) CrN/Cr/Si.

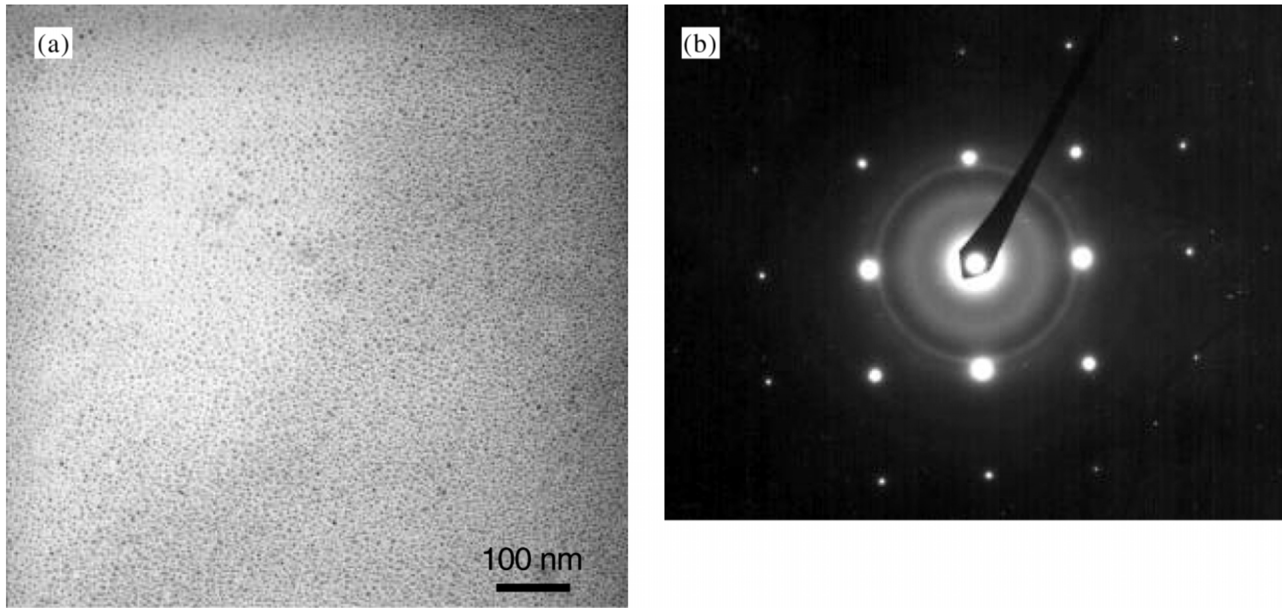

Fig. 4. (a) TEM micrograph of the MEVVA Cr deposited silicon showing the presence of a larger number of nano-scale Cr and (b) SAD pattern resulting from the MEVVA Cr deposited silicon showing diffraction rings on a background of single crystal silicon spots.

3.3. SIMS analysis

SIMS was conducted to elucidate the elemental distribution of chromium and nitrogen in the CrN films for CrN/Cr/Si and for CrN/Si assemblies. Fig. 3a,b shows the logarithmic intensities associated with chromium and nitrogen with silicon noise as a function of sputtering time for CrN/Si and CrN/Cr/Si assemblies, respectively: good quality films on the silicon substrates are observed. For instance, the acquired homogeneity is exhibited in the depth of the layers, showing similar intensity variations for CrN/Si and CrN/Cr/Si. The stoichiometric ratio of nitrogen and chromium in the CrN film cannot be changed significantly by the MEVVA Cr ion-implanted interlayer, as resolved from the SIMS depth profiles.

3.4. TEM observation

TEM was used to disclose the microstructure of the Cr interlayer by MEVVA. Fig. 4a,b shows the plan-view bright field image and selected area diffraction (SAD) pattern of the MEVVA Cr-deposited silicon wafer, respectively, implying the presence of a large number of nano-clusters (Fig. 4a) and a weak diffraction pattern (Fig. 4b) with a background of single crystal silicon spots, associated with the thin MEVVA Cr interlayer. The d-spacing calculated for the diffraction rings matches with the standard d-value of Cr [11]. The presence of such Cr diffraction rings proves that chromium disilicide ($CrSi_2$) was not formed here.

$CrSi_2$ can be directly synthesized using MEVVA techniques at a substrate temperature of 150 °C and a current density $\geqq 8.8\ \mu A/cm^2$ [7,12]. Nevertheless, both the current density ($6\ \mu A/cm^2$) and the substrate temperature (approx. 100 °C) used in the performed experiment are consistently lower than required, seemingly explaining why $CrSi_2$ could not be produced.

Although $CrSi_2$ can be synthesized by solid–state diffusion (thermal annealing) [13,14], no such phase could be detected after CrN was deposited by CAPD. The substrate temperature was ~350 °C while the CrN film were being deposited, so insufficient energy was provided for Cr atoms to react further with the Si substrate.

3.5. Residual stress analysis

The residual stresses of the CrN/Si and CrN/Cr/Si assemblies and the differences between them were evaluated and compared. Residual stress often exists in deposited films and originates from two major sources: one is the intrinsic stress that depends on a deposition parameter such as, ion bombardment energy and the other is the thermal stress that is caused by the different thermal expansion coefficients between the film and the substrate [15–18]. The residual stresses were determined experimentally by a scanning laser curvature method, and the curvature was further converted into stress using Eq. (1). The needed parameters are, $E_S = 130.2$ GPa, $\nu_S = 0.279$ [19], $t_S = 725\ \mu m$ and t_f is the corresponding thickness of the CrN film observed by SEM, 0.3 μm

Table 1
A comparison between CrN/Si and CrN/Cr/Si assemblies determined by XRD, SEM and in situ stress measurements

Specimens	Preferred orientation	CrN films thickness (μm)	Measured curvature (m^{-1})	Residual stress (GPa)
CrN/Si	CrN (220)	0.3	-0.16 ± 0.01	-8.02 ± 0.53
CrN/Cr/Si	CrN (220)	1.3	-0.24 ± 0.01	-2.77 ± 0.12

for CrN/Si and 1.3 μm for CrN/Cr/Si. The residual stresses for CrN/Si and for CrN/ Cr/Si are −8.0 GPa and −2.8 GPa, respectively, as shown in Table 1. The obtained stress levels are reasonable in comparison with the values in the literature (−2.9 to −8.8 GPa) [2,6,20,21].

The thermal stress of CrN (σ_{CrN}) can be estimated as follows [22]

$$\sigma_{CrN}=\frac{(\alpha_{CrN}-\alpha_{Si})\Delta T}{\left[\frac{\nu_{crN}-1}{E_{CrN}}+\frac{h_{CrN}(\nu_{CrN}-1)}{h_{Si}E_{Si}}\right]} \tag{2}$$

where α is the thermal expansion coefficient ($\alpha_{CrN}=2.3\times10^{-6}$ K^{-1}, $\alpha_{Si}=4.1\times10^{-6}$ K^{-1}); ν is the Poisson's ratio ($\nu_{CrN}=0.199$, $\nu_{Si}=0.279$); E is Young's modulus ($E_{CrN}=452$ GPa, $E_{Si}=130.2$ GPa); h is the thickness of the films and substrates, and ΔT is the difference between the deposition temperature and the room temperature. The thermal stress (σ_{CrN}) is only 0.3 GPa for depositing CrN deposition herein, contributing approximately 4% for CrN/Si and 12% for CrN/Cr/Si. Therefore, the residual stress is mainly the intrinsic stress.

Surprisingly, an MEVVA Cr interlayer can drastically reduce the residual stress in the CrN film. To estimate the magnitude of the reduction of stress, the reduction of stress $\Delta\ \sigma$ can be defined as,

$$\Delta\sigma=|(\sigma_{CrN/Cr}-\sigma_{CrN})/\sigma_{CrN}|\times100\% \tag{3}$$

where $\sigma_{CrN/Cr}$ and σ_{CrN} are the corresponding residual stress with and without the MEVVA Cr interlayer, respectively. The role of the Cr interlayer is apparent: it can significantly relax the residual stress of CrN films by up to 65%. It can therefore effectively reduce the residual stress in the growing of CrN films, using Eq. (3).

4. Conclusions

This study compared and characterized the microstructures and residual stress of CrN on a silicon wafer formed by CAPD both with and without a Cr intermediate layer deposited by MEVVA using XRD, SEM, TEM and SIMS.

1. No intermediate phases of $CrSi_2$ were formed between the MEVVA Cr and the Si substrate after MEVVA Cr implantation and subsequent CrN coating.
2. The diffraction patterns of the specimens indicated the presence of the CrN phase, with a (220) preferred orientation for both CrN/Si and CrN/CrN/Si.
3. The plan-view bright field TEM and its SAD reveal the presence of a large number of nano-clusters and a diffraction pattern with a background of single crystal silicon spots from the interlayer of MEVVA Cr.
4. The origin of the diffraction ring is a clear indication of the nano-crystalline Cr deposited by MEVVA.
5. Moreover, in situ stress measurements demonstrate that the presence of a Cr interlayer between CrN and Si can dramatically reduce the residual stress in CrN films.

Acknowledgments

The authors would like to thank the National Science Council of the Republic of China, for financially supporting this research under contract number of NSC 91PFA0400049. The Surftech Corporation, Taiwan is also highly appreciated for preparing the MEVVA Cr and CAPD CrN films. The authors would also like to thank Mr S.-S. Guo for his assistance in measuring the residual stresses.

References

[1] S. Han, J.H. Lin, S.H. Tsai, S.C. Chung, D.Y. Wang, F.H. Lu, H.C. Shih, Surf. Coat. Technol. 133–134 (2000) 460.
[2] M. Odén, C. Ericsson, G. Håkansson, H. Ljungcrantz, Surf. Coat. Technol. 114 (1999) 39.
[3] F.D. Lai, J.K. Wu, Surf. Coat. Technol. 88 (1996) 183.
[4] G. Brown, A. Anders, S. Anders, M.R. Dickinson, R.A. MacGill, E.M. Oks, Surf. Coat. Technol. 84 (1996) 550.
[5] S. Han, J.H. Lin, X.J. Guo, S.H. Tsai, Y.O. Su, J.H. Huang, F.-H. Lu, H.C. Shih, Thin Solid Films 377–378 (2000) 578.
[6] F.-H. Lu, H.-Y. Chen, Thin Solid Films 398–399 (2001) 368.
[7] H.N. Zhu, B.X. Liu, Appl. Surf. Sci. 161 (2000) 240.
[8] G.G. Stoney, Proc. R. Soc. Lond. Ser. A 82 (1909) 172.
[9] Powder Diffraction File, Joint Committee on Powder Diffraction Standard, ASTM, Philadelphia, PA, 1996, Card 11-0065.
[10] R.L. Boxman, S. Goldsmith, Surf. Coat. Technol. 57 (1992) 39.
[11] Powder Diffraction File, Joint Committee on Powder Diffraction Standard, ASTM, Philadelphia, PA, 1996, Card 06-0694.
[12] S. Wang, H. Liang, P. Zhu, Appl. Surf. Sci. 153 (2000) 108.
[13] J.O. Olowoafe, M.-A. Nicolet, J.W. Mayer, J. Appl. Phys. 47 (1976) 5182.

[14] E.G. Colgan, B.Y. Tsaur, J.W. Mayer, Appl. Phys. Lett. 37 (1980) 938.
[15] H. Windischmann, J. Vac. Sci. Technol. A9 (1991) 2431.
[16] J.A. Sue, A.J. Perry, J. Vetter, Surf. Coat. Technol. 68/69 (1994) 126.
[17] H. Oettel, R. Wiedemann, Surf. Coat. Technol. 76–77 (1995) 265.
[18] T. Matsue, T. Hanabusa, Y. Ikeuchi, Thin Solid Films 281–282 (1996) 344.
[19] W.A. Brantly, J. Appl. Phys. 44 (1973) 534.
[20] M.C. Bost, J.E. Mahan, J. Appl. Phys. 63 (1988) 839.
[21] W. Herr, E. Broszeit, Surf. Coat. Technol. 97 (1997) 335.
[22] W.D. Kingery, H.K. Bowen, D.R. Uhlmann, Introduction to Ceramics, John and Wiley, New York, NY, 1976, pp. 197–199.